Phoenix Upgrades in Support of Real-time Space Object Capture and Handoff at AMOS

Bryan Law, Dennis Liang, Tom Kelecy, Andrew Alday, Jake Barros, Paul Sydney, and John Africano
Air Force Maui Optical and Supercomputing Site,
Boeing LTS, 535 Lipoa Parkway, Ste 200, Kihei, HI 96753
dennis.liang.ctr@maui.afmc.af.mil

Paul, Kervin
Air Force Maui Optical and Supercomputing Site,
AFRL, 535 Lipoa Parkway, Ste 200, Kihei, HI 96753
paul.kervin@maui.afmc.af.mil

ABSTRACT

The increasing population of space objects orbiting the earth has motivated the development of Wide Field Of View (WFOV) optical sensors. The WFOV capability can significantly reduce the maximum time to search for and detect uncorrelated space objects over a specified region of the sky, and subsequently reduce revisit time. The timely capture and handoff of "lost" or newly discovered objects between sensors supports numerous space surveillance activities. The Air Force Maui Optical and Supercomputing (AMOS) site has refurbished a Baker-Nunn telescope (Phoenix) which has a 6.8° by 6.8° field-of-view (FOV) optical sensor. In addition, AMOS operates a Raven-class telescope with an approximate 0.7° by 0.7° FOV capable of producing sub arc-second metrics. This paper presents hardware and software upgrades that were made to the Phoenix telescope to support a near real-time state vector hand-off between sensors. The system performance requirements and calibration results are presented. The capture and hand-off performance results will be used to outline requirements for an operational implementation.

1. MOTIVATION AND BACKGROUND

There are over 9000 objects orbiting the earth that are tracked and cataloged on a regular basis [1]. It is estimated that there are over several hundred unique objects that are not cataloged, but are large enough to be tracked [Ed Barker, JSC, personal communications]. With limited tracking resources available for object-based surveillance tracking (go find a specific satellite), a WFOV capability would greatly alleviate the burden of capturing many of the un-cataloged objects, and better support a search and survey based (scan the sky and report what you find) tracking strategy that will become more pragmatic as the population of space objects increases.

In this environment, the ability to rapidly pass object tracking information between sensors will enable efficient implementation of a search and survey tracking strategy. Specifically, the concept of operations has a WFOV sensor "capturing" lost or new unknown objects, and passing those off to other sensors for follow-up tracking. The follow-up tracking sensors typically have narrower fields-of-view, but more accurate metrics. It should be noted that the narrow FOV does impose a requirement on the handoff accuracy. Ultimately, high accuracy follow-up tracking will allow orbit characterization leading to cataloging of the objects. Rapid capture and characterization of uncorrelated space objects will be enabled by a global network of high accuracy metric sensors such as the High Accuracy Network Determination System (HANDS) presently being deployed [2].

2. SENSORS DESCRIPTION

The initial acquisition telescope, Phoenix, is a modified-Schmidt telescope with a 78 cm primary mirror, and a focal ratio of f/1 with a 50 cm aperture. The Baker-Nunn design was incorporated into twelve telescopes used in the Smithsonian Astrophysical Observatory's satellite tracking network from 1957 to 1975. The Phoenix telescope is located at the Remote Maui Experiment (RME) site in Kihei, Maui. Initially designed for film photography on 55.6

mm high speed films, the original Baker-Nunn telescope has been retrofitted with a 4k × 4k CCD array and a field flattening lens which provides a 6.8˚ × 6.8˚ FOV. The drive and control systems were also refurbished to allow the telescope to perform semi-autonomous, autonomous, or remote operations. The WFOV nature of the newly automated Baker-Nunn telescope not only makes it ideal for satellite tracking, but also ideal for efforts in the searching and tracking of orbital debris, asteroids, and comets.

The sensor being handed off to, AMOS Raven, follows a design paradigm which utilizes commercially available hardware and software products resulting in an autonomous system with flexible configurations and upgrade paths, as well as reduced production and maintenance costs. The telescope has been operating nearly autonomously at AMOS since 2001 atop Haleakala, on Maui, HI, providing the U.S. Air Force Space Command with high accuracy space track observations (metrics) for deep-space satellites in the Space Surveillance Network (SSN). AMOS Raven design utilizes an f/3 Newtonian Torus Optics telescope with a 0.37 m diameter primary mirror and a Finger Lakes Instrumentation MaxCam CM2-1 with 13 micron pixels. A Software Bisque MME German-Equatorial mount and the Sky software package control telescope pointing for all of the Raven systems. Observation data metrics are derived through astrometric image processing where the line-of-sight to the satellite is computed by comparing the satellite location to the background stars in the CCD image. Raven has undergone various upgrades since its inception to improve metric quality to the arc-second level.

3. PHOENIX UPGRADES

Part of the Phoenix upgrade includes retrofitting a high quantum efficiency (QE), back-illuminated Fairchild CCD486 4k x 4k array with 15µm x 15µm pixels, in its imaging camera. While technical issues with the array packaging delayed integration of the camera containing the CCD486 array, a surrogate front-illuminated 4k x 4k array was used with Phoenix. Having resolved issues causing the delays, the camera containing the CCD486 array was ready for installation in July 2005. The back-illuminated CCD486 array has greater than 90% QE over the visible band, compared to about 50% QE offered by the surrogate array. The post-upgrade Phoenix has a limiting magnitude of about 16.5 in the visible. Several hardware and software enhancements were planned to occur at the same time as the camera installation to address performance issues and add new system functionalities in support of the hand-off efforts.

Previous metric calibration has shown that Phoenix is capable of producing metric residuals within 10 arc-seconds. However issues inherent in the optical system are causing optical aberrations and introducing difficulties in obtaining consistent metric processing and results.

The original Baker-Nunn optical prescription produces an image plane free of comatic aberration on a curved surface having a Petzval radius of approximately 520 mm. There are several approaches to reducing the Petzval curvature. One method includes modifying the Schmidt corrector triplet in combination with additional optics in the converging beam which are required to balance aberrations such as spherical aberration and coma. The aperture of the Schmidt corrector is 20 inches and 4 out of the 6 surfaces are general aspheres, therefore the cost of modifying the corrector is high. The simplest and least expensive approach is to introduce a flat field lens near the image plane to reduce the Petzval sum while having minimal impact on third order aberrations and chromatic aberration. Since the Baker-Nunn optical system is F/1 the beam approaches the image plane at 45 degrees. Introducing any glass in the beam will contribute to aberrations. The flat field lens must replace the detector window and be mounted as close as possible to the image plane. The CCD486 array used in the Phoenix system produces a 62mm x 62 mm wide or 87 mm diagonal image plane. The flat field lens was required to extend beyond the footprint of the chip itself to clear the wire bonds which resulted in an 11 mm center thickness flat field lens. The flat field lens was designed as a plano-convex lens with the plano or optically flat surfaces towards the image plane. The wire bonds extended above the chip by 0.007” therefore the flat field lens was separated from the CCD sensor by 0.010”. The close proximity of the flat field lens, also functioning as the vacuum window, introduced additional heat load on the sensor. A Cryo-Tiger refrigeration system was incorporated to cool the CCD camera.

Due to the thickness of the flat field lens and separation from the image plane, third order aberrations were introduced. The prescription for the lens was designed to balance spherical aberration, coma, and field curvature resulting in the best possible solution producing 60 micron spot sizes. A single element flat field lens has limitations but it was the least expensive and the simplest to implement. The flat field lens was required to have a certain

radius, thickness and bevels to form a vacuum seal with the camera vacuum housing. The original spot size of the Baker-Nunn was 40 microns coma free on a curved image plane of radius 520 mm.

After the camera and flat field lens were installed in the retrofitted Phoenix, the first light images exhibited a certain amount of coma. The Schmidt system should produce a coma free image even with the addition of the flat field lens near the image plane. Therefore the primary mirror was adjusted to reduce the spacing between the corrector and the Schmidt sphere. The corrector is required to be precisely located at the center of curvature of the Schmidt sphere to eliminate coma and astigmatism. After making a series of small adjustments to the corrector and mirror spacing the camera was refocused to the new image plane. After a few iterations the degree of coma could be seen to decrease as the mirror was brought closer to the corrector or "stop". The 31 inch diameter primary mirror was raised within its cell closer to the corrector until there was no further travel. It was determined that the only way to reduce the separation further would be to machine the flange of the telescope section holding the corrector lens. This corrector lens cell section has a 7/8 inch thick top flange where the corrector lens is fastened on top.

Extensive optical models were performed to simulate the performance of the Phoenix optical system. The optical models included every possible combination of system mis-alignment to determine the cause of the observed coma. The conclusion was that the system "stop" was not in the correct axial location by approximately 12 mm. The Phoenix system is a refurbished Baker-Nunn instrument. This set of Baker-Nunn instrument which Phoenix is based on changed hands several times and was ultimately sold at a government auction as a lot of 4 Baker-Nunn sets. There was no record of all the mechanical hardware for each set of Baker-Nunn and there were discrepancies found between the hardware and original drawings dated in the 1960's. Neither were there any records to indicate whether every Baker-Nunn was made with the exact same curvature primary mirror. The conclusion was that the corrector lens cell section could safely be machined to reduce the thickness of the flange by 3/8 inch, bringing the primary mirror closer to the "stop".

After machining the section flange, Phoenix was reassembled for observations. These new images agreed with optical models that were performed. Coma was minimized and the spot size was reduced by approximately 25 to 40% near the edge of the 9.8 degree diagonal field of view.

Software changes to the Phoenix and Raven system were minimized to simplify future integration into operational systems. For Phoenix, the operator used an existing capability to manually identify handoff targets in the image, whose angular position was computed from "in frame" astrometric processing. A simple orbit determination package was created to convert metric observations into the AFSPC Two Line Element (TLE) Set file. For AMOS Raven, a test version of the Raven software was created with the added capability of realtime monitoring a handoff directory for high priority "Ad Hoc" tasking. The tasking was initiated by the presence of TLE files in the handoff directory and the Raven dynamic scheduler inserted the TLEs as new high priority tasked satellites. In general, this handoff object, if visible, was scheduled immediately after its TLE file was transferred into the handoff directory.

4. PHOENIX TO RAVEN HANDOFF

A key objective of this test was to demonstrate how easily the technology necessary to implement a real-time handoff could be integrated into Space Surveillance systems. The operational AMOS Raven system typically tasks objects using a dynamic scheduler where the next highest priority visible satellite is selected for tracking after the currently tasked observations are complete. This dynamic scheduling accommodates weather outages and "Ad Hoc" tasking. For this test, a modified version of the Raven software that incorporated real-time monitoring of a "handoff" directory was tested. New handoff TLEs copied to this "handoff" directory were treated as "high priority Ad Hoc" tasking priorities, resulting in the immediate scheduling and observation of the handoff objects of interest. Thus, normal Air Force Space Command (AFSPC) are allowed to continue previous scheduled operations with only occasional, brief interruptions to accommodate a tasked handoff. The rapid response of follow up sensors is necessitated by the accuracy of the initial orbit determination affecting the orbit prediction accuracy of the Hand-off TLE.

The handoff test between Phoenix and Raven occurred on February 15, 2006, on the island of Maui, HI (approximately 21° N latitude and 156° W longitude). The pass geometry is depicted in Fig. 1 where each of the

objects was moving south to north over the handoff period. The Phoenix sensor is located near sea level in Kihei on the south coast of Maui, while Raven is located about 19 km away atop Haleakala at a little over 3 km altitude.

The handoff process as implemented for this test involved a combination of automated and manual functions. The handoff process is shown in Fig. 2, and begins with Phoenix image acquisition of a "serendipitous" object. Pairs of images separated by approximately 1 minute are taken, and immediately analyzed for detection of uncorrelated objects in the sensor FOV.

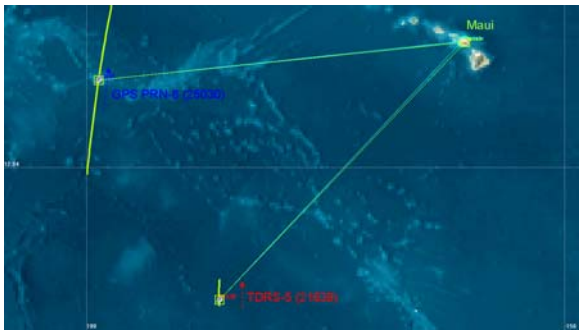

Fig. 1: Phoenix to Raven handoff geometry.

The image analysis is done using AstroGraph, an "in-frame" astrometric processing tool, and the right ascension and declination "metrics" are derived for the object of interest as identified in each of the images. If multiple objects are detected in close proximity to each other in either of the frames, a strategy must be applied to determine which pair is correlated.

Once derived, the resulting metric pairs of measurements are then passed to the initial orbit determination and a state vector of the object at an epoch corresponding to one of the measurement times is then passed to the acquiring sensor, in this case, Raven.

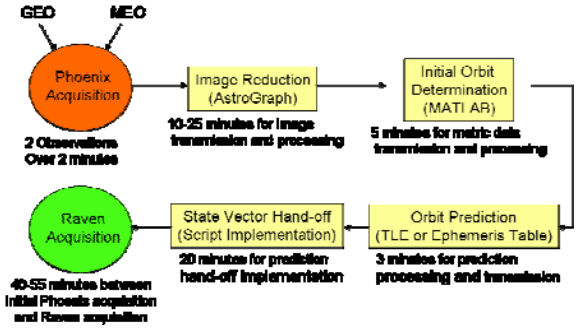

Fig. 2: Phoenix to Raven handoff processing sequence, with processing functions and nominal processing times.

5. INITIAL ORBIT DETERMINATION

The AMOS sensors best accommodate pointing acquisition of space objects through tasking and implementation of Two-line Element Sets (TLEs). In general, a set of orbital parameters can be determined from three sets of measurements using one of many techniques (e.g. Gauss' method). This is sometimes easier said than done, in particular when attempting to determine orbits of geosynchronous objects over relatively short periods of time. However, one can facilitate an orbit approximation over a "local" period of time from two measurements which is adequate for handoffs over relatively short periods of time. Two pairs of measurements can thus be processed to produce a "circular orbit approximation" that will suffice in accuracy when propagated over the period between initial data acquisition and handoff acquisition. This approach has been demonstrated by others [3] with some success on both geosynchronous (GEO) and geosynchronous transfer orbit (GTO) objects. Successful orbit capture and characterization will require accurate follow-up measurements, and application of a sufficiently more sophisticated technique.

The handoff timeline from Phoenix data acquisition through Raven re-acquisition for the TDRS-5 GEO object (COSPAR# 91054 / SSN# 21639) covered a period of about 58 minutes, and is shown at the bottom of Fig. 3. Though it appears most of the time is taken up by the manual process of porting the resulting TLE to the Raven system, right around 29 minutes, most of this time was in fact due to waiting for weather to clear. The "sneaker netting" was necessary because of the segregation between the Phoenix and Raven systems, though the actual amount of time to transfer took only a matter of minutes. An operational configuration reduces this to seconds as the TLE can be passed via file transfer protocol (ftp). Next largest time allocation is the 26-27 minutes needed to detect the object and reduce the metrics. This part of the process was also done manually, though it too can be automated. The total handoff process can thus potentially be reduced to a matter of minutes.

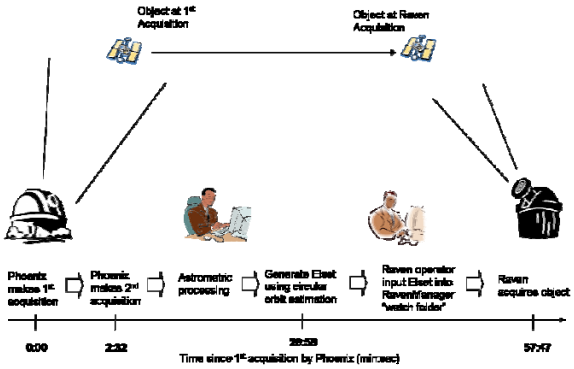

Fig. 3: TDRS-5 initial Phoenix data acquisition to Raven re-acquisition timeline.

The handoff timeline for the GPS PRN-8 (COSPAR# 97067A / SSN# 25030) MEO (semi-synchronous orbit) object took about 43 minutes, and is shown at the bottom of Fig. 4. As was the case for the TDRS-5 object, most of the total time is taken up by the porting the TLE to the Raven system, in this case around 26 minutes. Again, weather was a factor in the delay of hand-off acquisition. The metric detection and processing took around 14-15 minutes. As previously mentioned, with automation the total process can be reduced to a matter of minutes.

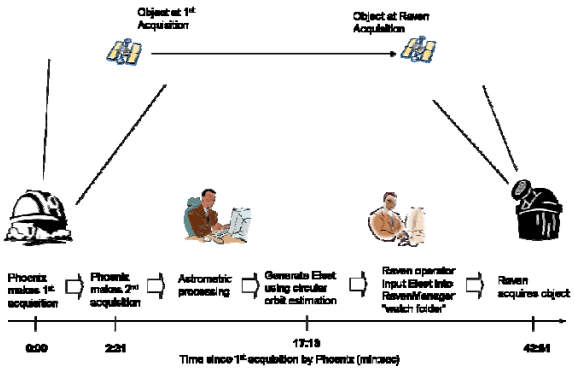

Fig. 4: GPS PRN-8 initial Phoenix data acquisition to Raven re-acquisition timeline.

Two aspects of performance were considered in this work. The first was the quality of the measurements as determined by a measurement calibration process. The second, and key to the goal of this work, was the quality of the handoff in terms of pointing errors at acquisition. This second performance metric is a function not only of the acquisition measurement quality, but also of the fidelity of the initial orbit determination and subsequent orbital propagation using the SGP4 algorithm.

The measurement accuracy is a factor that will affect the quality of the initial orbit determination and subsequent propagation. The initial Phoenix measurements were "calibrated" according to the process outlined in Fig. 5. The known reference orbit for each of the objects is used to compute reference right ascension and declination metrics at the measurement time that can then be compared to the actual measurements. TDRS calibration metrics have been previously shown to be good to ~0.3 arc-second or better. The operations version of the Goddard Trajectory Determination System (OPSGTDS) tool was used in the calibration process.

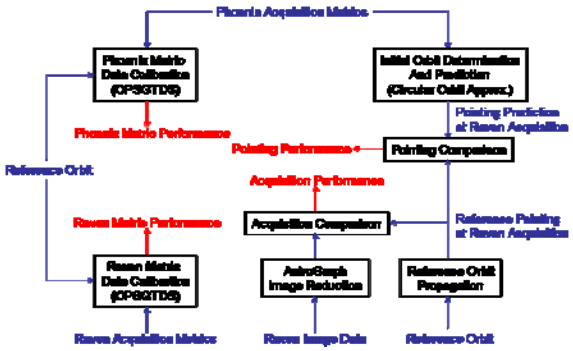

Fig. 5: Metric calibration and handoff analysis processes.

The calibration metric residuals for the initial Phoenix measurement pairs taken for each of the two objects are shown in Table 1. The TDRS-5 measurements are seen to be good to arc-second level, while the GPS PRN-8 are accurate over the range of 10-32 arc-seconds. The reason for the lower quality of the GPS initial measurements might be the proximity of the object in the Phoenix sensor FOV at acquisition. Further analysis shows it to be near the edge where distortion becomes a larger factor.

Phoenix Acquisition Metric Calibration Accuracy					
SSN	YYYYMMDD	HHMM	SS.SSSS	RA (as)	DEC (as)
21639	20060215	851	23.082	7.2994	0.778
21639	20060215	853	54.7421	-13.1813	-1.6099
25030	20060215	925	37.3828	2.1449	10.8666
25030	20060215	928	8.1054	-20.0035	-32.2471

Table 1: TDRS-5 and GPS PRN-8 Phoenix acquisition calibration metric residuals.

The metric data pairs were used to initialize the orbit state for each of the objects. The states were translated to the TLE format and passed to the Raven sensor for attempted acquisition. The pointing and propagation performance results are presented in the next section.

6. HANDOFF MEASUREMENT RESULTS

The calibration metric residuals for the Raven re-acquisition measurement pairs taken for each object are shown in Table 2. Several measurements were taken on each to validate the acquisition. The 5 TDRS-5 calibration residuals are at the arc-second level, while the 4 GPS PRN-8 residuals are a few arc-seconds in accuracy. It should be re-emphasized that the residuals in Table 2. represent measures of accuracy relative to the known "truth" orbits.

Raven Re-acquisition Metric Calibration Accuracy					
SSN	YYYYMMDD	HHMM	SS.SSSS	RA (as)	DEC (as)
21639	20060215	949	9.7149	1.2294	1.8758
21639	20060215	949	23.3164	0.9143	1.7977
21639	20060215	949	36.8671	1.1631	1.9485
21639	20060215	949	50.4179	0.8992	1.7288
21639	20060215	950	4.0546	0.9723	1.7211
25030	20060215	1008	27.8554	3.4348	4.1284
25030	20060215	1008	41.4609	2.9267	3.2353
25030	20060215	1008	55.2304	2.9404	3.4322
25030	20060215	1009	8.8398	3.6782	3.4391

Table 2: TDRS-5 and GPS PRN-8 Raven re-acquisition calibration metrics.

The pointing offsets at acquisition relative to the predicted location at acquisition time are presented in Table 3. These offsets are the right ascension and declination differences between the Raven sensor FOV center and where the object appeared at each image capture time. The TDRS-5 offsets are at the 1 arc-minute level, whereas the GPS PRN-8 offsets are a little over 21 arc-minutes. The radial FOV for Raven is right around 21-29 arc-minutes (0.35°-0.48°), hence this object was at or near the edge of the image around the time of acquisition.

Object SSN	Time (h:m:s)	RA Ctr (deg)	DEC Ctr (deg)	RA Obs (deg)	DEC Obs (deg)	RA Offset (arc-min)	DEC Offset (arc-min)
21639	9:49:07	118.165083	2.762444	118.2967	2.7799	7.897000	1.047333
21639	9:49:21	118.221583	2.767417	118.3535	2.7849	7.915000	1.049000
21639	9:49:34	118.277833	2.772417	118.4103	2.7899	7.948000	1.049000
21639	9:49:48	118.334000	2.777389	118.4669	2.7948	7.974000	1.044667
21639	9:50:02	118.390542	2.782417	118.5239	2.7998	8.001500	1.043000
25030	10:08:25	120.272458	47.120000	120.6465	47.4718	22.442500	21.108000
25030	10:08:39	120.396833	47.216750	120.774	47.5697	22.630000	21.177000
25030	10:08:53	120.522917	47.314778	120.9036	47.6689	22.841000	21.247333
25030	10:09:06	120.647583	47.411667	121.0324	47.7667	23.089000	21.302000

Table 3: TDRS-5 and GPS PRN-8 Raven acquisition pointing offsets.

7. SUMMARY AND FUTURE WORK

These handoff tests have shown that it quite feasible to handoff from a WFOV sensor with limited accuracy to a narrower FOV operational sensor, providing very accurate metric measurements. Initial orbit determination of deep space objects based on a few measurements and a circular orbit approximation still provides sufficient accuracy for reacquisition after an elapsed time of 30 to 60 minutes.

Future work will focus on several areas. The first objective is to simplify the handoff process, automating the detection, initial orbit determination, and TLE transmission of handoff targets from the WFOV to NFOV sensors. The second objective is to operate the WFOV sensor in a continuous, wide area search, producing and handing off targets as they are found. Third, assess the UCT tasking and processing with Air Force Space Surveillance Network (SSN). Finally, a future study should determine the operational limits of the system in terms of target orbit classes, hand off timelines, and geographically distributed sensors.

8. REFERENCES

1. Liou, J.-C., and N. L. Johnson, “Risks in Space from Orbiting Debris,” *Science*, 311: 340-341 January 20, 2006.
2. Kelecy, T. and C. Sabol, “Rapid Orbit Characterization and Real-time State Vector Handoff Using High Accuracy Metrics,” *AMOS Technical Conference 2006 Proceedings*, Sept. 5-9, 2005, Maui, HI.
3. Musci, R., T. Schildknecht, M. Ploner and G. Beutler, “Orbit Improvement for GTO Objects Using Follow-up Observations,” COSPAR 2004.

9. ACKNOWLEDGEMENTS

We wish to thank the Air Force Research Laboratory (AFRL), Det-15, for funding this work. We acknowledge the support provided by Kris Hamada, with Boeing-LTS on Maui, and Dan O’Connell, with hnuPhotonics